THE JOURNAL OF PHYSICAL CHEMISTRY B

ARTICLE

pubs.acs.org/JPCB

Direct Observation of a Dark State in Lycopene Using Pump-DFWM

Marie S. Marek, Tiago Buckup, and Marcus Motzkus*

Physikalisch-Chemisches Institut, Ruprecht-Karls-Universität Heidelberg, D-69120 Heidelberg, Germany

ABSTRACT: We apply pump-degenerate four-wave-mixing (pump-DFWM) for the investigation of the ultrafast internal relaxation of the excited states of lycopene. A unique feature in the pump-DFWM signal, appearing at small temporal delays between the initial pump pulse and the DFWM sequence, provides direct evidence for the participation of an additional excited state located between the S_2 and S_1 states. Our experimental findings are corroborated by a detailed numerical simulation of lycopene's pump-DFWM signal using the Brownian oscillator model. A very fast dynamics directly after excitation of the S_2 state manifests as a component populated with a time constant of about 20 fs and which decays to S_1 with a lifetime of 110 fs. This ultrafast dynamics is discussed under the light of several different models suggested for the relaxation pathway of carotenoids. In this context, we show that the dynamics can be explained in terms of a dark electronic state between the S_2 and S_1 states.

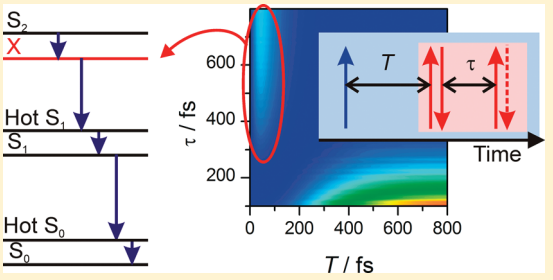

1. INTRODUCTION

Carotenoids are among the most abundant natural pigments and play a key role in photosynthetic light-harvesting complexes.[1] In this function, carotenoids are, e.g., responsible for the absorption of light in the green-blue region of the visible spectrum which is not accessible for (bacterio-)chlorophylls. In spite of the importance of carotenoids in photobiology, the dynamics of the excited states are still not clear.

So far, it is generally accepted that one-photon transition between the ground state S_0 ($1A_g^-$) and the first excited singlet state S_1 ($2A_g^-$) is symmetry forbidden. The lowest optically allowed excited state of carotenoids is the S_2 ($1B_u^+$) state. For the deactivation mechanism from the S_2 state, however, until now no model has been presented which is able to account for all experimental observations.

In this regard, the appearance of an additional long-living spectro-temporal feature on the lower-energy side of the S_0-S_2 absorption in transient absorption spectra has raised great debate. Recently, Niedzwiedzki et al.[2,3] discussed this so-called S* component as a different conformation of the S_1 state for xanthophylls and open-chain carotenoids, since long polyenes in solution generally show a distribution of conformational disorder. Both the deviations of the S_2-S_1 relaxation from the energy gap law[4] as well as additional time constants observed in several experiments could be explained by a branched relaxation into two states of nearly planar *cis* and *trans* conformation. For macro-carotenes, in contrast, the long-lived absorption signal of the S* component has been attributed to the absorption of a hot ground state,[5] which is populated by internal conversion from the S_1 state. This interpretation was supported by recent temperature dependent steady state absorption and ultrafast pump-supercontinuum-probe experiments on β-carotene.[6] Pump-deplete-probe experiments on several different carotenoids with conjugation lengths between 9 and 15 double bonds,[7,8] on the other hand, proposed a mechanism where the hot-S_0 is populated via stimulated impulsive Raman-scattering (ISRS) with the S_2 state as an intermediate step. The attribution of the S* signal to a hot ground state accounts for the red-shifted spectral position of this signal compared to the ground state absorption. Furthermore, comparison of transient absorption measurements following one- and two-photon excitation in apo-carotenes suggested the participation of a hot ground state in the relaxation pathway as well as the existence of at least two minima on the S_1 surface.[9,10] While both minima can be reached via one-photon excitation of a vibrationally hot-S_2, relaxation after one-photon excitation of the vibrationally cold S_2 and direct two-photon excitation of the S_1 state lead to two different minima on the S_1 surface.

More recently, theoretical consideration[11] concerning the signal generation in transient absorption showed that a signal of a hot ground state would appear as a negative component which contradicts the experimental findings.[7] A positive signal as it is observed in the experiments should only be obtained when fifth-order interactions are accounted for in pump−probe measurements. In these higher order processes, the pump electric field interacts already four times with the molecule, i.e., two-photon interaction, leading to an ISRS excitation as previously suggested by pump-depletion experiments.[7] Such a higher order process can be routinely observed in carotenoids even at moderate photon fluences ($\sim 10^{14}$ photons/cm^2) due to the resonant two-photon excitation ($S_0 \rightarrow S_2 \rightarrow$ hot-S_0) and the strong transition dipole moment of the hot-S_0-S_2 transition.

A second important aspect regarding the electronic states of carotenoids is the role of electronic dark states, i.e., singlet states which cannot be directly excited by one-photon transitions.

Received: March 24, 2011
Revised: May 10, 2011
Published: June 02, 2011

Calculations on short linear polyenes indicated the existence of one or two additional dark states between S_2 and S_1, depending on the conjugation length N of the carotenoid.[12,13] Hence, it has been proposed that these states of $3A_g^-$ and $1B_u^-$ symmetry may act as a coupling bridge in the S_2-S_1 relaxation step.[14−18] Time-resolved absorption spectroscopy indicated the involvement of the $1B_u^-$ state in the relaxation pathway of carotenoids with chain lengths up to $N = 10$ double bonds while in the longer pigments from $N = 11$ on the $3A_g^-$ state was observed.[16] Only recently the observation of strong oscillations at the early delay times in transients of lutein and β-carotene have been ascribed to a coupling of the S_2 state with another electronic dark state.[19] In this case, quantum chemical calculations predicted this dark state to be the $1B_u^-$ state.

Clarification of the carotenoids' ultrafast deactivation dynamics hence represents a very demanding field and requires more elaborate experimental techniques. The possibility of concurrent monitoring of population and coherence dynamics predestines the four-wave-mixing techniques for the investigation of such complex systems.[20−22] In these techniques with three laser beams, the first two light−matter interactions stem from different pulses in contrast to transient absorption. This allows for control of the temporal delays between all three interactions and hence decouples the temporal and spectral resolutions of the experiment. Applied to β-carotene, the method of two-dimensional spectroscopy allowed for detailed analysis of the excited state absorption signal in a spectral region where the signals from ground state bleach and stimulated emission overlap strongly.[11] The experimental results of this study gave no evidence for any excited state between S_2 and S_1 but suggested the existence of an excited state absorption of the S_2 state in the visible spectral range. Similar results have been obtained in degenerate four-wave-mixing (DFWM) studies which so far exclusively support the simple relaxation model including only S_2 and S_1.[23−29]

The lack of any direct observation of transient dynamics of dark states with DFWM may be, however, explained by the fact that DFWM is not exclusively sensitive to the pure excited state dynamics, since the signal always has a contribution of the ground state as well. Thus, a combination of the two mentioned techniques, transient absorption and DFWM, seems to be perfectly suited for the investigation of the excited state dynamics of carotenoids. In previous works,[24,30,31] we applied such a combination, namely, pump-DFWM, to examine the dynamics of β-carotene's excited states. Pump-DFWM is a two-dimensional technique, where the system is promoted to the excited state by an initial pump pulse prior to the DFWM sequence. In these works, we showed that pump-DFWM is able to give information about both the electronic dynamics and the dephasing behavior as well as frequencies of vibrational modes involved in the relaxation of the excited state.[30] Furthermore, pump-DFWM allows for analyzing the dynamics of the carotenoid's vibrational modes with high spectral and temporal resolution.[31] Due to the additional spectral axis, the population and depopulation of the individual modes in time can be studied in detail as well as the process of internal energy redistribution in the respective electronic states. Apart from carotenoids,[24,25,30−32] pump-DFWM has also been used for the investigation of halogens[33,34] or bimolecular systems like $Na + H_2$.[35]

In this paper, we apply pump-DFWM to lycopene and thus expand our knowledge to open-chain carotenoids. In a detailed investigation, we especially address the question of the participation of a hot ground state in the deactivation network in the context of a signal appearing at early delays between the initial pump pulse and DFWM sequence. Our picture is finally completed by a theoretical model simulation of the experimental signal which strongly supports the involvement of an additional excited state in the relaxation after excitation of S_2.

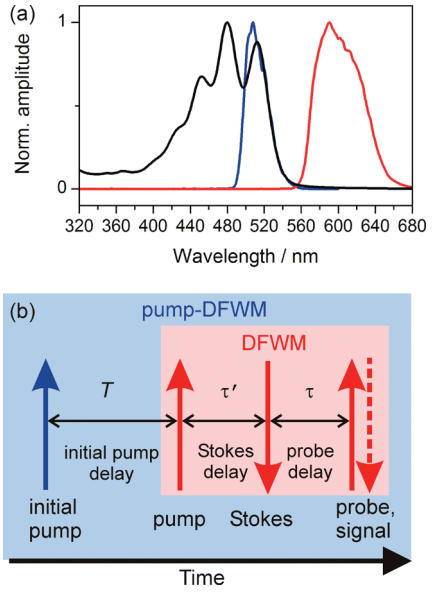

Figure 1. (a) DFWM (red line) and initial pump (blue line) spectrum together with lycopene's ground state absorption spectrum (black line) in THF. The so-called "*cis*-peak" at 360 nm is almost completely absent. (b) Time ordering of the incident pulses in the pump-DFWM experiments.

2. MATERIALS AND METHODS

2.1. Sample Preparation. *All-trans*-lycopene was used as received from Roth and dissolved in THF (HPLC grade) under an argon atmosphere. The optical density of the sample was adjusted to OD 1.5 at lycopene's first maximum of absorption near 512 nm (Figure 1a). During the measurement, the irradiated volume (thickness $d = 500$ μm) was exchanged continuously using a peristaltic pump to avoid any undesirable accumulation effects. The solution showed no sign of sample photodegradation over the course of the experiment.

The absence of a "*cis*-peak" at 360 nm in Figure 1a shows that the amount of *cis*-isomer in the sample was very low. The possible role of sample impurities was cross-checked by performing the experiments with lycopene samples with higher *cis*-isomer content. No modification of time constants or enhancement or suppression of the pump-DFWM signal features discussed in this paper were observed. Moreover, due to the quadratic dependence of the DFWM signal on the molecule concentration, our experiment is mainly sensitive to major components and insensitive to impurities. For example, a 10% impurity would be responsible for just 1% of the total DFWM signal for comparable transition dipoles.

2.2. Experimental Setup. The basic experimental setup has been described in detail previously.[30,31] In short, the DFWM sequence was generated in a single stage home-built noncollinear optical parametric amplifier (nc-OPA) by splitting its output into three parts of equal intensity.

The DFWM spectrum was centered at 600 nm (Figure 1a). Hence, it is not resonant with the S_0-S_2 transition but resonant with the excited state absorption of S_1 and its vibrationally excited manifold (hot-S_1).[36] After compression, the DFWM pulse duration was 13 fs at the position of the sample. The pump and Stokes energies were in the range 10−12 nJ, and the energy of the probe was 7 nJ. The initial pump (IP) pulse was generated in a second nc-OPA, and the spectrum was centered at 510 nm. After compression, the IP pulse reached the sample with typical energies of 30 nJ and pulse durations below 15 fs. The excitation energy corresponds to a fluence of 9.8×10^{14} photons/cm^2 per pulse which results in 15% of the excited molecules in the focal volume. A computer-controlled shutter blocking the initial pump allowed for recording a nonresonant DFWM transient without the presence of the initial pump as a reference for each pump-DFWM transient. All four excitation beams, namely, the initial pump and the three DFWM beams, were focused using the same concave mirror (f = 30 cm). The beams were aligned in a folded BOXCARS arrangement.[35]

The relative delay between the four pulses was controlled by two separate computer-controlled piezo stages (Figure 1b). The initial pump preceded the DFWM sequence by T. The delay τ' between the pump and Stokes of the DFWM sequence was kept at zero in all measurements. The delay between the Stokes and probe pulse is called the probe delay τ. While the system evolves freely along the T-axis similar to the pump−probe delay in transient absorption measurements, the transient grating induced by the first two pulses in the DFWM sequence evolves with τ. Hence, by varying τ and T, pump-DFWM allows for monitoring of electronic and structural dynamics simultaneously in one experiment. Typical measurements were performed varying the probe delay τ and the initial pump delay T followed by plotting τ vs T in a 2D graph (Figure 3). Each τ vs T scan was averaged four times, with 40 laser shots per data point. The pump-DFWM signal was detected by photomultipliers at chosen wavelengths using a 10 nm bandwidth interferometric filter.

2.3. Pump-DFWM Signal Analysis. A typical pump-DFWM signal consists of a nonoscillatory and an oscillatory contribution. The electronic population dynamics of the electronic states under investigation manifests itself in the nonoscillatory part of the signal, while the oscillatory contribution mainly contains information on the molecular wavepacket frequencies and dephasing times. It is important to note that the pump-DFWM signal always has a contribution of the nonresonant ground state DFWM. This contribution becomes significant when the DFWM spectrum is near resonance with the ground state absorption. In our case, however, the DFWM spectrum was completely off resonant to lycopene's ground state absorption and the ground state DFWM contribution was negligible (Figure 1a). Hence, the analysis of the different contributions of the pump-DFWM signal was much simplified and the residual pure nonresonant DFWM signal measured without the presence of the initial pump was used to improve the signal-to-noise ratio by subtracting it from the pump-DFWM signal. Next, the DFWM transient was cut at τ = 100 fs in order to exclude the electronic peak at time zero. It is important to note that by cutting the initial 100 fs of the DFWM transient no information about population dynamics along the delay T is neglected. The slow nonoscillatory contribution was then fitted with an exponential decay and subtracted from the transient, leaving only the oscillatory contribution. A fast Fourier transformation (FFT) was finally performed using zero-padding and apodization[37] in order to obtain vibrational power spectra.

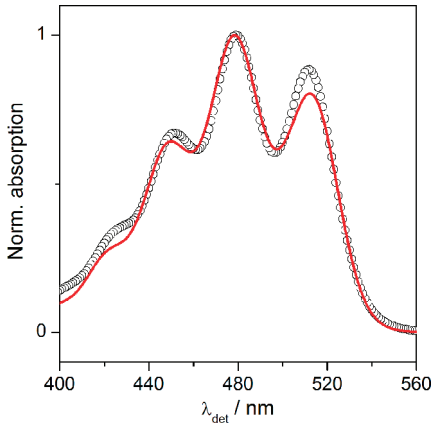

Figure 2. Experimental (black dots) and simulated (red line) linear absorption spectrum of lycopene. For the simulation of the absorption spectrum, two molecular vibrations (1517 cm^{-1}, 1141 cm^{-1}) as well as a low frequency mode at 250 cm^{-1} were used. The dephasing times were 1.97 ps, 1.42 ps, and 20 fs and the relative amplitudes had a ratio of 0.75:0.5:4, respectively.

2.4. Numerical Simulations. Lycopene's pump-DFWM signal is calculated treating pump-DFWM as DFWM on the excited state. The effect of the initial pump pulse was accounted for by a shift of 15% of population from the ground state to the S_2 state prior to the interaction with the DFWM sequence. Using a numerical rate model for the relaxation pathway (section 4.2, Figure 8), the population flow during the initial pump delay time T was estimated. The simulation of the DFWM signal is based on the framework introduced by Mukamel.[38] Application of the rotating wave approximation, neglecting the spectral bandwidth assuming degenerate excitation and approximation of the pulses by δ-functions, leads to an expression for the DFWM signal $S(\tau',\tau)$ depending on the response function $R(t_3,\tau,\tau')$:

$$S(\tau',\tau) = \int_0^\infty dt_3 \left| \left(\frac{i}{\hbar}\right)^3 R(t_3,\tau,\tau') \right|^2 \qquad (1)$$

The total response function is composed of the individual response functions of all possible processes which add coherently to the signal. The expressions for the individual response functions scale with the population dynamics in the particular electronic state whose evolution in time τ is described by the rate models discussed in section 4.2 (Figure 8). Apart from the population dynamics, the response functions also scale with the four transition dipole moments μ of the specific electronic transitions playing a role in the processes. Additionally, the response functions depend on the respective line broadening function $g(t)$ of the vibrational modes. The expression for $g(t)$ is derived from the multimode Brownian oscillator model[38] and is given by the sum over all contributions $g_j(t)$ of the individual oscillators:

$$g(t) = \sum_j g_j(t)$$

$$g_j(t) = \xi_j^2 \int_0^t d\tau_1 \int_0^{\tau_1} d\tau_2 C_j'(\tau_2) + i\xi_j^2 \int_0^t d\tau_1 \int_0^{\tau_1} d\tau_2 C_j''(\tau_2) \qquad (2)$$

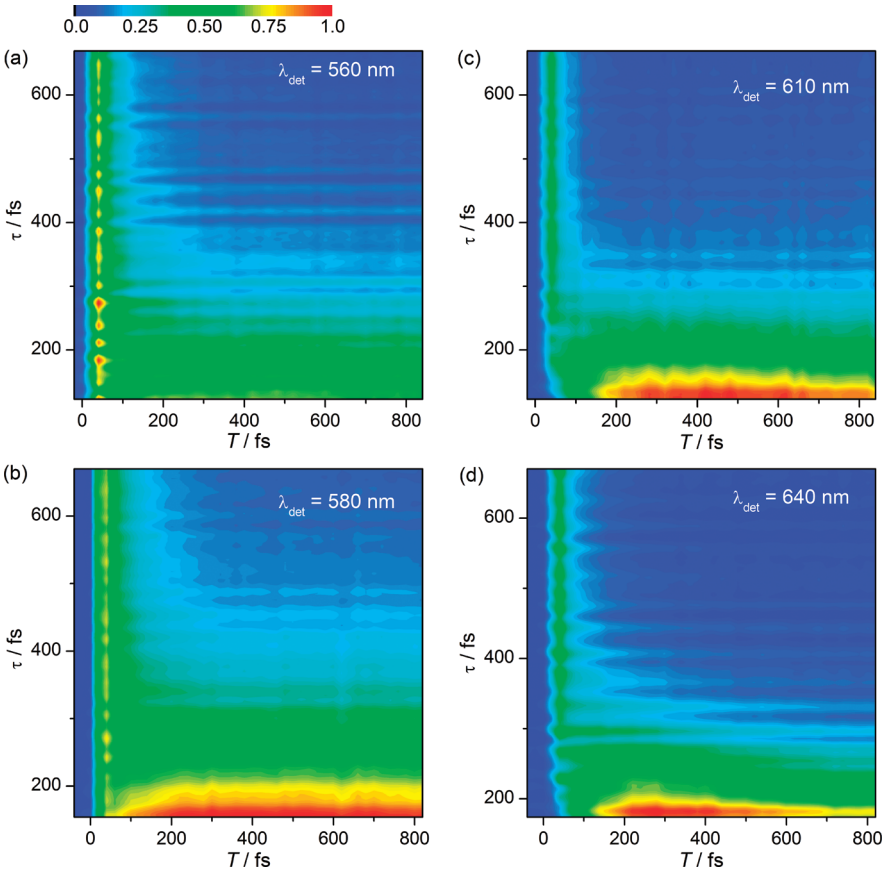

Figure 3. 2D plots of the pump-DFWM transients in the probe delay τ against the initial pump delay T for different detection wavelengths.

Here, ξ_j is the individual mode's amplitude. The correlation functions C_j' and C_j'' are defined as

$$C_j''(t) = -\frac{\hbar}{2m_j\zeta_j}\exp\left(\frac{-\gamma_j t}{2}\right)\sin(\zeta_j t) \tag{3}$$

$$C_j'(t) = \frac{\hbar}{4m_j}\frac{1}{\zeta_j}\left[\coth\left(\frac{i\phi_j'\hbar\beta}{2}\right)\exp(-\phi'_j t) - \coth\left(\frac{i\phi_j\hbar\beta}{2}\right)\exp(-\phi_j t)\right] - \frac{2\gamma_j}{m_j\beta}\sum_{n=1}^{\infty}\frac{\nu_n\exp(-\nu_n t)}{(\omega_j^2+\nu_n^2)^2-\gamma_j^2\nu_n^2} \tag{4}$$

with $\zeta_j = [\omega_j^2 - (\gamma_j^2/4)]^{1/2}$, $\phi_j' = (\gamma_j/2) - i\zeta_j$, $\phi_j = (\gamma_j/2) + i\zeta_j$, and $\nu_n = (2\pi/\hbar\beta)n$. The other variables are ω_j which is the mean frequency, γ_j which is the damping constant $1/T_{2,j}$, the reduced mass m_j, and β that stands for $1/k_BT$.

Using the line broadening function (eq 2), the linear absorption spectrum of lycopene can be calculated.[38] In Figure 2, the calculated spectrum is shown together with the experimentally measured one of lycopene in THF. The good agreement of both spectra shows that the chosen method for calculating $g(t)$ is sufficient for the description of lycopene's signal.

3. EXPERIMENTAL RESULTS

In the pump-DFWM experiments, the two delays τ (probe delay) and T (initial pump delay) are varied. This 2D transient data is shown in Figure 3 for several detection wavelengths ranging from the blue edge (560 nm) of the S_1 absorption to the far red edge (640 nm). This perspective allows for the observation of the deactivation network as well as the structural dynamics. Along the T axis, Figure 3 shows for all detection

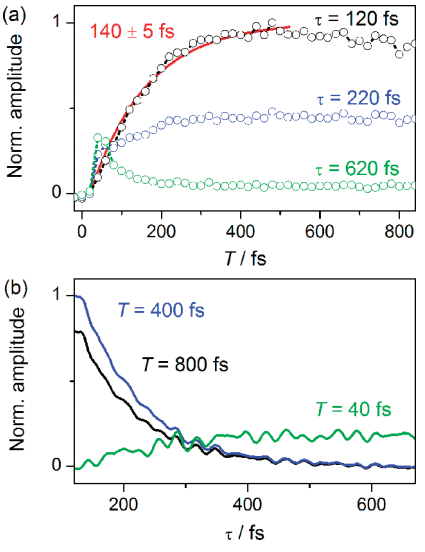

Figure 4. (a) Pump-DFWM transients in the initial pump delay T at different probe delays τ. (b) Pump-DFWM transients in the probe delay τ at different initial pump delays T. The detection wavelength was 610 nm.

dx.doi.org/10.1021/jp202753j |J. Phys. Chem. B 2011, 115, 8328–8337

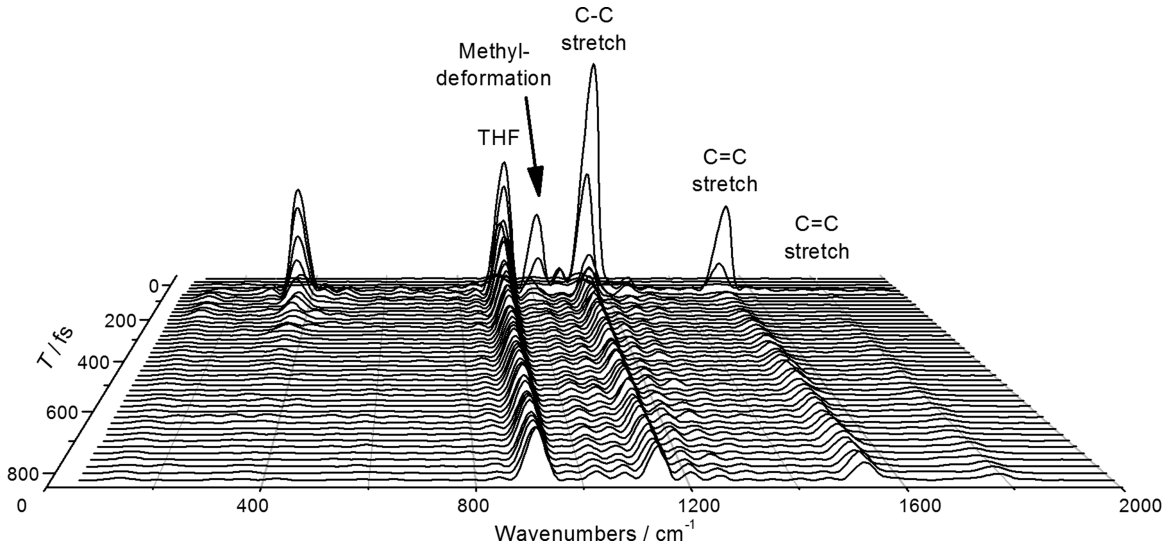

Figure 5. FFT power spectra of lycopene for different initial pump delays T at a detection wavelength of 570 nm.

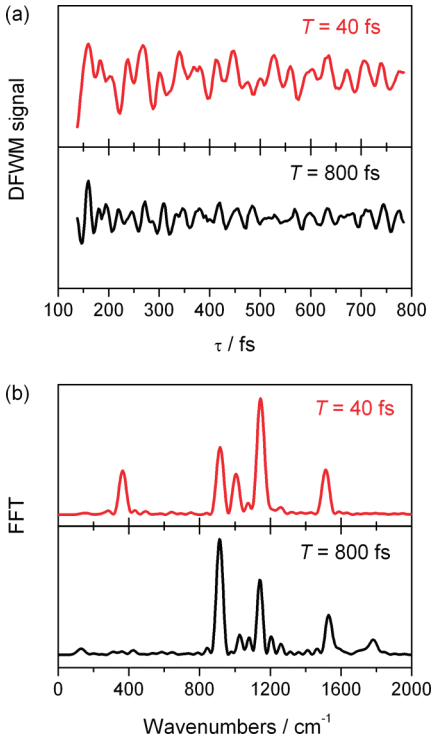

Figure 6. (a) Oscillatory part of the DFWM transients and (b) FFT spectra of the transients at λ_{det} = 570 nm of the signal at T = 40 fs (red) and the vibrationally relaxed S_1 signal at T = 800 fs (black).

wavelengths a slow rise of the signal at small probe delays τ. This rise is emphasized in Figure 4a by means of a cut along the T axis and correlates with the deactivation of S_2 and the flow of population into the S_1 state. Exponential fitting gives a rise time of 140 fs. Along the other axis of Figure 3, the delay τ between the DFWM probe pulse and the temporally overlapped pump and Stokes is shown (Figure 4b). In this direction, the oscillatory and nonoscillatory contributions of the DFWM signal emerge. For initial pump delays larger than T = 100 fs, the expected exponential decay of the slowly varying component of the signal in τ is visible. At early delays T from 10 to 80 fs (maximum at T = 40 fs), however, a rising signal occurs with a long lifetime in τ (>2 ps). This component is stronger at blue-detuned detection wavelengths (560 nm) than at red-detuned detection wavelengths (640 nm).

The characteristics of such a unique feature at early initial pump delays T followed by a signal rising in T can be observed in the development of the FFT spectra as well. In Figure 5, the FFT spectra obtained at a detection wavelength of 570 nm are shown for initial pump delays T between 0 and 800 fs. The assignment of the oscillating wavepackets to molecular vibrations is similar to that of β-carotene.[30,31] At T = 800 fs, the two solvent modes at 915 and 1080 cm^{-1} are clearly visible as well as the methyl deformation at 1030 cm^{-1}, the C—C and C═C stretching modes at 1140, 1205, and 1530 cm^{-1}, and a C═C mode at 1800 cm^{-1}.[39,40] The two C═C modes at 1530 and 1800 cm^{-1} rise with T from T = 100 fs on. In previous experiments, this behavior was attributed to the process of vibrational cooling in the S_1 state, which is completed at 400 fs in β-carotene.[31,40] However, the vibrational spectra for early delays T show several differences compared to T = 800 fs. In a small time window of the first 100 fs, a component at 370 cm^{-1} is observed that vanishes at later initial pump delays. The C═C stretching mode at 1800 cm^{-1} on the other hand is absent in the spectra at early delays T.[40] Furthermore, the vibrational modes visible at all delays T have different frequencies at T = 40 fs compared to T = 800 fs. The methyl deformation mode is shifted from 1030 cm^{-1} at T = 800 fs to 1007 cm^{-1} at T = 40 fs and the stretching mode from 1530 to 1513 cm^{-1}, respectively.

4. DISCUSSION

4.1. Interpretation of the Experimental Results. Comparison of the pump-DFWM results for different initial pump delays T revealed a completely different behavior of the signal for IP delays of about T = 40 fs than for later delays. The pump-DFWM signal at delays T from 100 fs on has only one major contribution, which can be well explained in terms of the population flow from the initially excited S_2 state to S_1 including vibrational cooling. Since the DFWM spectrum is not resonant to the S_2-S_m

transition, the signal at small delays T is only weak. For later T, the signal begins to rise while the electronic population reaches the Franck−Condon window defined by the spectral properties of the DFWM sequence. The signal shows a rise in T with a time constant of 140 fs which resembles time constants found in transient absorption measurements that are generally attributed to the lifetime of the S_2 state (130 fs).[41] The signal at T = 40 fs, however, does not fit into this simple picture. Several aspects of this signal require further analysis.

The most remarkable characteristic of the signal at T = 40 fs is the long lifetime of the nonoscillatory contribution (2.5 ps). While the signal appears only in a very narrow time window along the T-axis, its lifetime in τ is even much longer than the lifetime of the signal at later T delays corresponding to the S_1 state (2.5 ps compared to ∼100 fs at T = 800 fs). This long lifetime in τ is also apparent in the oscillatory contribution of the pump-DFWM signal. In Figure 6a, only the pure oscillations, i.e., the nonoscillatory contribution was subtracted, are compared for T delays of 40 and 800 fs. At 40 fs, the high frequency oscillations have larger amplitude and much longer dephasing times (∼500 fs) than at later delays (∼200 fs at T = 800 fs). Note that the solvent mode at 915 cm^{-1} which dephases much slower contributes strongly to the signal and dominates the late part of the transients (from τ = 500 fs on). The signal at T = 40 fs hence must stem from an electronic state with a lifetime different from the S_1 state.

Another important aspect in the investigation of electronic states is the respective normal modes. Cuts through the FFT spectra in Figure 5 show that the S_1-specific C═C stretching mode at 1800 cm^{-1} is completely absent at T = 40 fs but is distinctly visible in the spectra at later delays (Figure 6b). This point again emphasizes that the spectra at early initial pump delays cannot originate from the S_1 state.[30,31,40] Moreover, it is important to note that the individual frequencies of the modes at early IP delays lie closer to the corresponding frequencies of the ground state DFWM spectra than to the ones of the S_1 modes at T = 800 fs. The frequency of the methyl deformation mode, for example, is shifted from 1007 cm^{-1} at T = 40 fs which resembles the mode of the S_0 state at 1012 cm^{-1} to 1030 cm^{-1} at T = 800 fs. The same applies for the stretching mode at 1513 cm^{-1} for early delays, which agrees better with the S_0 mode at 1505 cm^{-1} than with the S_1 mode at 1530 cm^{-1}.

The unique signal at T = 40 fs appears during the relaxation process from the initially excited S_2 to S_1, but on the basis of only these two states, its mentioned characteristics cannot be explained. At this early T delay, the S_1 state is weakly populated and thus cannot contribute decisively to the signal. Note that the DFWM signal depends on the squared population difference (Δn^2) between the involved states, and at early delay times, the S_1 state has an almost negligible population. The S_2 state on the other hand is instantaneously populated by the initial pump pulse which makes it difficult to explain the delay of 40 fs with respect to the excitation. Hence, understanding the origin of this feature might be the key for differentiating between the several models discussed for the carotenoids' relaxation pathways.

One of these models predicts the existence of several geometric isomers of the carotenoids either already in the ground state[11,42] or via photoexcitation in the S_1 state.[2] In the latter case, both S_1 isomers are populated by S_2 with the same rate constant in a branched relaxation pathway.[2,3] Hence, this model clearly cannot explain the appearance of the long-living signal at T = 40 fs. If the signal originated from an S_1' state populated concurrently with S_1, then why should it arise much earlier and

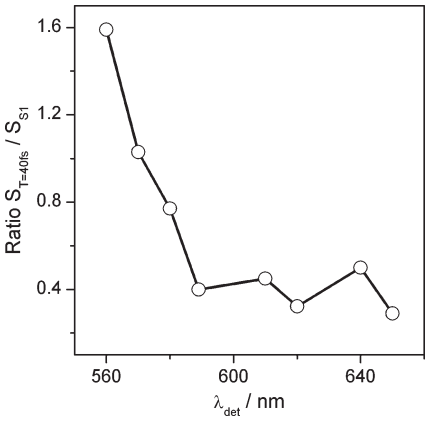

Figure 7. Relative contribution of the long-living signal taken at T = 40 fs as compared to the vibrationally relaxed S_1 signal at T = 600 fs.

in a much smaller time window than the S_1 signal? A similar argument discards the model of different isomers already in the ground state for an explanation of the signal.[11] In this model, S_1 and S_1' are populated from different S_2 states. A time constant for the S_2'-S_1' transition was not determined. However, even if this relaxation step takes place fast enough to account for an S_1' signal appearing already at T = 40 fs, the completely different evolutions of the S_1' and S_1 signals remain unexplained. Since both states in this model are assumed to be S_1 states, their electronic properties should be similar and hence their temporal characteristics are expected to be comparable. Thus, the S_1' signal should in this case overlap with the S_1 signal in the T direction and not vanish completely after 80 fs. Finally, the absence of the S_1 specific mode at 1800 cm^{-1} in the FFT spectra of the signal at T = 40 fs is strong evidence for this signal not stemming from S_1 or any kind of electronic state with similar structural characteristics.

A second model can be rationalized if one takes a closer look at the pump-DFWM data in Figure 3. A comparison of the four graphs shows that the relative amplitude of the signal at 40 fs and at later T is strongly dependent on the detection wavelength. To make this dependence more obvious, Figure 7 shows that the signal at T = 40 fs compared to the S_1 signal at T = 600 fs becomes stronger the more the detection is shifted toward the first ground state absorption maximum at 512 nm. A very similar behavior of the pump-DFWM signal of β-carotene was observed in our previous work,[30] where the long-living signal was identified with a signal of a vibrationally excited ground state. In this context, this hot-S_0 state is excited by the DFWM sequence from the S_2 state via a process called stimulated emission pumping DFWM (SEP-DFWM).[43] Such an assignment readily accounts for the observed features of the signal at T = 40 fs. A hot ground state signal clearly would be more prominent when the signal is detected close to the ground state absorption maximum, which corresponds to blue-detuned detection wavelengths in DFWM. Generally, an increasing contribution of a signal at early T for smaller wavelengths could also be explained by a DFWM signal between S_2 and a higher lying electronic state S_m, when the S_2-S_m transition lies in the spectral region around 500 nm. In this case, however, the signal would be expected to live much shorter in τ, as the electronic lifetimes of such highly excited states are rather in the sub-ps range. The lifetime of lycopene's hot ground state on the other hand is determined to be about 6 ps.[7] Therefore, a SEP-DFWM mechanism between S_2 and hot-S_0 hence can rationalize

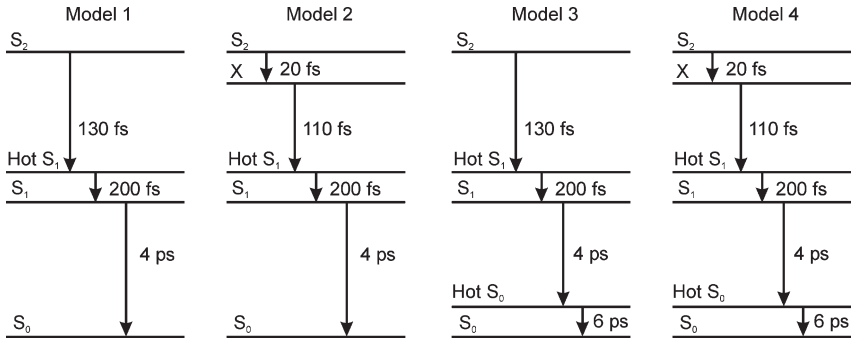

Figure 8. Four rate models tested in the simulations of lycopene's pump-DFWM signal. Only with model 4 it was possible to reproduce the experimental signal. The time constants of the electronic lifetimes and vibrational cooling are obtained by exponential fitting of the experimental data or from the literature (hot-S_0).

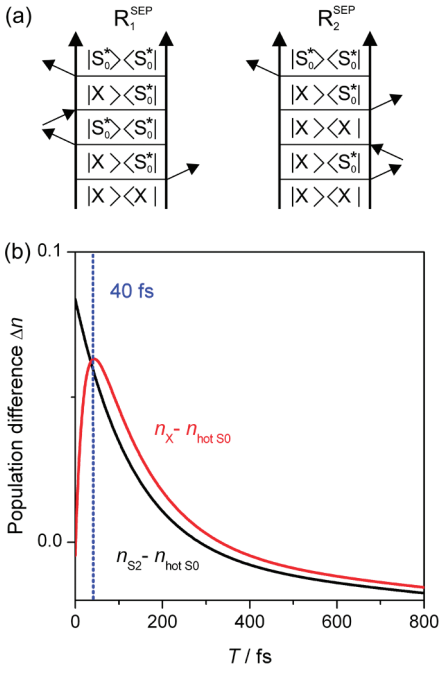

Figure 9. (a) Stimulated emission pumping (SEP) DFWM mechanism between an electronically excited state X and hot-S_0 (S_0^*) needed to reproduce the pump-DFWM signal's temporal evolution at early initial pump delays T. (b) Evolution of the population difference Δn between S_2 and hot-S_0 (black) as well as X and hot-S_0 (red) in time.

the long lifetime in τ. The lifetime of hot-S_0 also accounts for the longer dephasing times of the oscillations, whose frequencies moreover match with the ground state molecular modes, as discussed above. Along the T-axis, in contrast, the SEP-DFWM signal has only a short lifetime, since the starting point of the SEP process is the excited state population near the Franck−Condon region. The signal can only be stimulated as long as this excited state is sufficiently populated, which is the case during the first 100 fs of the initial pump delay T. However, the signal's exact position of 40 fs along the T-axis is not intuitive and requires further investigation.

A third model based on the participation of one or more additional excited states ($3A_g^-$, $1B_u^-$) can assist in the interpretation of the signal at early delay times.[15,19] In this case, the long-living signal at T = 40 fs observed in our experimental data could in principle be thought of as a signal of an additional excited state directly below the S_2 state. Precondition for this situation would be a very fast relaxation from the S_2 state to the additional dark state. This model will prove its utility in section 4.2, where the simulation of lycopene's pump-DFWM signal is discussed.

4.2. Simulation of the Pump-DFWM Signal. The assignment of the long-living feature at early initial pump delays to a hot ground state signal so far is based on the interpretation of a third-order nonlinear signal with many contributions. By means of Feynman diagrams, one can estimate that about 80 different processes in principle can contribute to the pump-DFWM signal of a carotenoid. Hence, for an unambiguous interpretation of the signal, a numerical simulation is indispensable. We simulated lycopene's pump-DFWM signal using different rate models describing the relaxation pathway (Figure 8) after excitation to S_2.

In the previous section, we discussed the unique features of the signal at T = 40 fs. The main challenge of the simulations was to find a process accounting for all these characteristics: (1) Such a process must lead to a signal with a long lifetime in τ but rapidly decay in T before the S_1 signal arises. (2) It has no amplitude at T = 0 fs but rises very fast to its maximum at T = 40 fs, meaning that the signal does not appear instantaneously after excitation of the S_2 state. Apart from these requirements, the simulations must also reproduce the validated contributions from other studies such as the S_1 signal.

In order to obtain the simplest possible model reproducing our transient signal, we first started implementing a very elementary model including only S_2 and S_1 states (model 1 in Figure 8). For simplicity, only one vibrationally excited level of the S_1 state was included, which is necessary to reproduce the effect of vibrational cooling responsible for the decaying signal at large T. With this model, the experimental signal for large initial pump delays (T > 100 fs) was well reproduced. However, before T = 100 fs, the signal had no amplitude at all and no long-living feature at 40 fs appeared, since the only contribution was the (hot) S_1 signal that cannot arise before the population has reached the S_1 manifold. Introduction of an additional electronic state between S_2 and S_1 (model 2) gave essentially the same results. Hence, we included a vibrationally hot ground state in our model (model 3 in Figure 8). Simply including this level in the rate model had no effect on the simulation results. The signal at the beginning of the T axis still had no amplitude, since any DFWM process between the hot ground state and S_2 scales with the population of the hot ground state. Right after excitation, no population has reached this low lying state and the hot-S_0

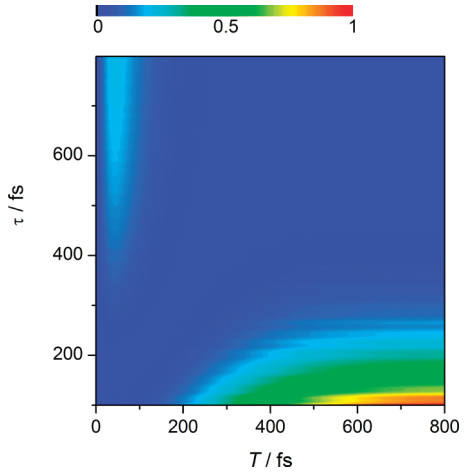

Figure 10. Results of the simulation of lycopene's pump-DFWM signal shown as a 2D plot of probe delay τ vs initial pump delay T. The ratio of the transition dipole moments of the included processes was hot-S_1-S_n:S_1-S_n:hot-S_0-X 1:2:1.1, respectively. The individual states' lifetimes are listed in Figure 8. For the oscillatory contribution, the prominent Raman modes of lycopene observed in Figure 5 (1800, 1530, 1140, and 1030 cm^{-1}) were included.

population thus is very small. The initial pump spectrum used in our experiment (Figure 1a) covers a range of 30 nm and hence could trigger an S_2-hot-S_0 stimulated emission. However, even accounting for this possibility by transferring a small percentage (1.5%) of population into hot-S_0 did not lead to a signal at early T delay.

More successful in generating such a signal was the introduction of a SEP-DFWM[43] process between S_2 and hot-S_0. In this case, the process starts in S_2 and therefore scales with the S_2 population which is largest directly after the interaction with the initial pump. The pump-DFWM signal in this simulation showed a long-living signal along τ with a large amplitude at $T = 0$ fs which decayed very fast in T before the typical S_1 signal at larger T appeared. This behavior can be understood quite easily, since the process of SEP-DFWM can simply be seen as DFWM starting at the upper state instead of the lower one. When the DFWM process between hot-S_0 and S_2 is considered as well as SEP-DFWM between S_2 and hot-S_0, the amplitude of the resulting signal exclusively depends on the squared population difference between the two states (Δn^2). The evolution of this population difference in T is shown in Figure 9b, and it is clearly seen that it has a maximum value at $T = 0$ fs and then decays.

The key for reproducing the long-living signal at 40 fs, and not at $T = 0$ fs, hence is the introduction of a SEP-DFWM process between two states whose population difference has a maximum at $T = 40$ fs. For this purpose, it was necessary to establish model 4 of Figure 8 where an additional state energetically directly below the S_2 state is populated with a time constant of 20 fs. The generally accepted S_2 lifetime of 130 fs is then composed of two steps with the lifetime of the additional state amounting to 110 fs.

With the SEP-DFWM mechanism taking place not between S_2 and hot-S_0 but between X and hot-S_0 (Figure 9a), it was now possible to reproduce the rising and slowly decaying component at $T = 40$ fs. The population difference between these two states is zero at time $T = 0$ fs and rises very rapidly to its maximum value at $T = 40$ fs (Figure 9b). The results of the simulations using model 4 are depicted in Figure 10 by means of a 2D τ vs T plot.

The simulated pump-DFWM signal reproduces qualitatively the prominent features of the experimental data shown in Figure 3. The rise along T delays of the signal in Figure 10 at early delays τ is composed of the lifetime of the X state (110 fs) and the process of vibrational cooling in S_1 (200 fs). The latter process is also mirrored in the fast exponential decay of the transients in the τ direction at delays T from 150 fs on until 800 fs. In the experiment, the time constants of this decay depend strongly on the detection wavelength similar to pump-DFWM experiments on β-carotene.[30] The shorter decay times for detection at larger wavelengths than the S_1 absorption maximum at 575 nm can be explained by the shorter lifetimes of the vibrationally excited levels of S_1. At small wavelengths, the vibrationally hot-S_n levels also lead to short decay times. Thus, the individual transition dipole moments vary depending on the detection wavelength in the experiment. The simulations, on the other hand, display integration over all wavelengths due to the approximation of the laser pulses as δ-functions. Hence, a compromise had to be found for the transition dipole moments of all contributing processes. For a better agreement between simulations and experimental data, it would be necessary to include the real spectral bandwidth of the DFWM pulses into the calculations, which will be undertaken in future.

A further aspect that has to be mentioned is the possibility of two-photon processes triggered by the initial pump pulse.[11,42] After populating the S_2 state, the IP could subsequently pump a fraction of the S_2 population either to a higher lying S_m state or to the hot-S_0. Both processes could only be distinguished by the lifetime of the DFWM signal in τ. Previous simulations of other experiments allude to the importance of an interaction between S_2 and S_m.[11,26,28,42] Implementation of an S_2-S_m transition in combination with population of S_m by the IP in our simulations finally allowed us to completely rule out this transition for the origin of the long-living signal. The signal of an S_2-S_m transition again scales with the population of S_2 and hence has a maximum at $T = 0$ fs, decaying with the S_2 lifetime in T and not peaking at 40 fs. At this point, it might be suggested that the shift of 40 fs observed in the experiment could be an effect of the finite IP pulse duration, which is neglected in our simulations based on δ-functions for the excitation pulses. If the second step of the IP process, where the population is pumped to S_m, is triggered by a later tail of the IP pulse than the first step of populating S_2, such a signal would be delayed from $T = 0$ fs. However, the pulse duration in our experiment was not longer than 15 fs, which can hardly account for a delay of 40 fs. Moreover, pump-DFWM experiments on β-carotene[30] and lutein (not shown) showed the same long-living feature but at initial pump delays of about 100 fs, which definitely cannot be caused by ~15 fs pulses. Nevertheless, a DFWM signal at the correct initial pump delay would be possible when an X-S_m transition was included. However, in the simulations, such a signal shows a very short lifetime in τ because of the short lifetimes obtained for X and S_m. Though the lifetime of S_m is not directly known, it is not expected to be longer than the 110 fs of X, as S_m is a highly excited singlet state.[44]

As a final remark of this section, we will address the issue of impulsive stimulated Raman scattering (ISRS) which leads to the population of the hot ground state in transient absorption measurements.[7,45] Such a kind of population mechanism has been intensively discussed recently and can play a role in pump-DFWM experiments. In the case of carotenoids, ISRS would lead to a higher population in the hot ground state after interaction with the IP. Since the relative amplitude of the long-living signal

at T = 40 fs depends on the population difference Δn between X and hot-S_0, the signal gets even larger when the possibility of stimulated emission to hot-S_0 is neglected. Our simulations therefore do not allow for a direct confirmation of such a process playing a role in lycopene and other carotenoids. However, the experimentally observed dependence of the relative signal amplitude on the probe wavelength (Figure 7) suggests that the SEP mechanism takes place in a spectral regime where ISRS would also be expected. Further experimental investigation in order to clarify the effect of ISRS thus would be very interesting and will be done in a future work. Especially the dependence of the individual contributions of the pump-DFWM signal on the energy and spectrum of the initial pump should give evidence of the role of this process.

4.3. What is X? The question naturally arising from our experimental and simulation results is whether this "X state" really is an electronic state. The initial pump pulse used in our experiments (Figure 1a) had enough intensity in the blue spectral region to possibly excite a vibrationally hot-S_2 state. The fast decay from S_2 to X in the simulations therefore could represent vibrational cooling in S_2 or, more generally, the approach of a Franck−Condon window for the S_2-hot-S_0 transition. A resonance enhanced transition is only possible as long as the S_2 state is populated and the Franck−Condon window to the hot ground state is accessible. In this case, however, the temporal position of the hot ground state signal would be expected to depend on the position of the S_2 electronic hypersurface where the wavepacket is created and thus to depend on the spectrum of the initial pump pulse. However, measurements in lycopene using red-shifted initial pump excitation spectra (λ = 525 nm, $\Delta\lambda$ = 15 nm ≡ 570 cm^{-1}) showed exactly the same long-living signal at T = 40 fs. Furthermore, pump-DFWM measurements of β-carotene where the initial pump pulse spectrum overlaps only with the transition to the vibrationally cold S_2 state show the same long-living hot-S_0 signal at initial pump delays of 100 fs.[31] Simulations of β-carotene's pump-DFWM signal (data not shown) also require this X state but with a population constant of about 80 fs.

The X state in our model thus actually seems to be an additional excited state between S_2 and S_1. Our simulations indicate that relaxation from S_2 to X takes place extremely fast (20 fs), while X has a lifetime of 110 fs. Such an intermediate state was already suggested in other experimental investigations.[17,19,46,47] Subpicosecond absorption spectroscopy in carotenoids with varying conjugation lengths suggested the intermediate state in lycopene to be of $3A_g^-$ symmetry.[16] The lifetimes of S_2 and $3A_g^-$ were determined to be 20 and 150 fs, respectively, which are in good agreement with our results. In femtosecond time-resolved absorption and Kerr-gate fluorescence experiments on different β-carotene homologues, an additional state located between S_2 and S_1 was necessary to explain the behavior of the S_2 relaxation rates depending on the conjugation length.[46] In this case, however, the authors assigned the longer lifetime of about 100 fs to the S_2 state and explained the identical rise time of S_1 with a very fast S_x-S_1 relaxation (10 fs). A long lifetime for S_2 (100−170 fs, depending on the solvent) and a shorter one for an intermediate state were also found in a recent femtosecond transient absorption study of lutein and β-carotene.[19] For the intermediate state, determined by quantum chemical calculations as $1B_u^-$, population time constants of 80 and 50 fs were obtained for lutein and β-carotene, respectively. Moreover, the authors ascribed the observation, that the fluorescence spectra of these carotenoids differ from a direct mirror image of the absorption, to the existence of the intermediate state. This means that the generally accepted S_2 lifetime of 130 fs in lycopene, which is normally determined either by fluorescence or via the rise time of the S_1 excited state absorption, is not necessarily the real lifetime of S_2 but may also include an intermediate relaxation step to an electronic state located energetically directly below. Whether the longer lifetime is assigned to S_2 or to the intermediate state seems to depend on the applied theoretical model. This ambiguity and the fact that the intermediate state does not have a strong absorption might be the reason why it is so difficult to observe this state in spectroscopic studies using transient absorption and DFWM. However, we showed that the intermediate state has an intense stimulated emission that leads to a unique signal in pump-DFWM. Such a stimulated emission of a nominally dark electronic state is possible due to the energetically proximity of the S_2 and X intermediate states. This leads to a symmetry breaking and a strong mixing character, which is experimentally apparent in the deformation of the fluorescence spectra compared to the ground state absorption.[19] This contrasts to the dark S_1 state: It is energetically separated from the higher lying states, possibly reached via a conical intersection, and shows a defined A_g^- symmetry. Therefore, the S_1 state shows no emission at all. In contrast to transient absorption, which is "blind" to such ultrafast stimulated emission during the deactivation of S_2 toward S_1, pump-DFWM hence can distinguish between these S_2 and X states close to each other and allows for an unambiguous assignment of the lifetime of 110 fs to the lower one.

5. CONCLUSIONS

The application of pump-DFWM to the investigation of the ultrafast dynamics in lycopene provides a comprehensive picture of its initial relaxation network. Analysis and simulation of the pump-DFWM signal provided strong evidence for an additional excited singlet state between S_2 and S_1 playing a role in the deactivation pathway. This state is populated extremely fast (∼20 fs) from the initially excited S_2 state and then relaxes with a time constant of ∼110 fs, which sums up to the time constant generally ascribed to the S_2 relaxation (130 fs). After this first rapid relaxation step, the temporal evolution of lycopene's pump-DFWM signal is predominantly determined by the vibrationally hot species of S_1 and S_0. These results show that pump-DFWM is much better suited for the investigation of such complex molecular systems than pure DFWM on the electronic ground state, as the very fast dynamics directly after excitation cannot be resolved in DFWM transients. The additional time axis in pump-DFWM, however, allows for the observation even of very fast processes right after photoexcitation with unrivaled resolution. Applied to carotenoids, it can thus distinguish between the dynamics of the S_2 state and other excited states which are energetically very close.

AUTHOR INFORMATION

Corresponding Author

*E-mail: marcus.motzkus@pci.uni-heidelberg.de. Phone: (+49)-6221548727. Fax: (+49)6221548730.

ACKNOWLEDGMENT

We thank Philip Kraack, Jens Möhring, and Torsten Krause for valuable discussions and Marco Hill for his technical support during the experiments. Support by the Fonds der Chemischen Industrie is gratefully acknowledged.

REFERENCES

(1) Polívka, T.; Sundström, V. *Chem. Rev.* **2004**, *104*, 2021.
(2) Niedzwiedzki, D. M.; Koscielecki, J. F.; Cong, H.; Sullivan, J. O.; Gibson, G. N.; Birge, R. R.; Frank, H. A. *J. Phys. Chem. B* **2007**, *111*, 5984.
(3) Niedzwiedzki, D. M.; Sullivan, J. O.; Polívka, T.; Birge, R. R.; Frank, H. A. *J. Phys. Chem. B* **2006**, *110*, 22872.
(4) Englman, R.; Jortner, J. *Mol. Phys.* **1970**, *18*, 145.
(5) Andersson, P. O.; Gillbro, T. *J. Chem. Phys.* **1995**, *103*, 2509.
(6) Lenzer, T.; Ehlers, F.; Scholz, M.; Oswald, R.; Oum, K. *Phys. Chem. Chem. Phys.* **2010**, *12*, 8832.
(7) Wohlleben, W.; Buckup, T.; Hashimoto, H.; Cogdell, R. J.; Herek, J. L.; Motzkus, M. *J. Phys. Chem. B* **2004**, *108*, 3320.
(8) Buckup, T.; Savolainen, J.; Wohlleben, W.; Herek, J. L.; Hashimoto, H.; Correia, R. R. B.; Motzkus, M. *J. Chem. Phys.* **2006**, *125*, 194505.
(9) Pang, Y.; Fleming, G. R. *Phys. Chem. Chem. Phys.* **2010**, *12*, 6782.
(10) Pang, Y.; Jones, G. A.; Prantil, M. A.; Fleming, G. R. *J. Am. Chem. Soc.* **2010**, *132*, 2264.
(11) Christensson, N.; Milota, F.; Nemeth, A.; Sperling, J.; Kauffmann, H. F.; Pullerits, T.; Hauer, J. *J. Phys. Chem. B* **2009**, *113*, 16409.
(12) Tavan, P.; Schulten, K. *J. Chem. Phys.* **1986**, *85*, 6602.
(13) Tavan, P.; Schulten, K. *Phys. Rev. B* **1987**, *36*, 4337.
(14) Rondonuwu, F. S.; Watanabe, Y.; Zhang, J. P.; Furuichi, K.; Koyama, Y. *Chem. Phys. Lett.* **2002**, *357*, 376.
(15) Furuichi, K.; Sashima, T.; Koyama, Y. *Chem. Phys. Lett.* **2002**, *356*, 547.
(16) Fujii, R.; Inaba, T.; Watanabe, Y.; Koyama, Y.; Zhang, J. P. *Chem. Phys. Lett.* **2003**, *369*, 165.
(17) Cerullo, G.; Polli, D.; Lanzani, G.; De Silvestri, S.; Hashimoto, H.; Cogdell, R. J. *Science* **2002**, *298*, 2395.
(18) Marian, C. M.; Kock, S. C.; Hundsdorfer, C.; Martin, H. D.; Stahl, W.; Ostroumov, E.; Müller, M. G.; Holzwarth, A. R. *Photochem. Photobiol. Sci.* **2009**, *8*, 270.
(19) Ostroumov, E.; Muller, M. G.; Marian, C. M.; Kleinschmidt, M.; Holzwarth, A. R. *Phys. Rev. Lett.* **2009**, *103*, 108302.
(20) Siebert, T.; Maksimenka, R.; Materny, A.; Engel, V.; Kiefer, W.; Schmitt, M. *J. Raman Spectrosc.* **2002**, *33*, 844.
(21) Siebert, T.; Schmitt, M.; Grafe, S.; Engel, V. *J. Raman Spectrosc.* **2006**, *37*, 397.
(22) *Ultrashort Laser Pulses - Generation and Application*; Kaiser, W., Ed.; Springer-Verlag: Berlin, 1993; Vol. 60.
(23) Oberlé, J.; Jonusauskas, G.; Abraham, E.; Rullière, C. *Chem. Phys. Lett.* **1995**, *241*, 281.
(24) Hornung, T.; Skenderovic, H.; Motzkus, M. *Chem. Phys. Lett.* **2005**, *402*, 283.
(25) Namboodiri, V.; Scaria, A.; Namboodiri, M.; Materny, A. *Laser Phys.* **2009**, *19*, 154.
(26) Christensson, N.; Polívka, T.; Yartsev, A.; Pullerits, T. *Phys. Rev. B* **2009**, *79*, 245118.
(27) Fujiwara, M.; Yamauchi, K.; Sugisaki, M.; Gall, A.; Robert, B.; Cogdell, R. J.; Hashimoto, H. *Phys. Rev. B* **2008**, *77*, 205118.
(28) Sugisaki, M.; Yanagi, K.; Cogdell, R. J.; Hashimoto, H. *Phys. Rev. B* **2007**, *75*, 155110.
(29) Christensson, N.; Chabera, P.; Hiller, R. G.; Pullerits, T.; Polivka, T. *Chem. Phys.* **2010**, *373*, 15.
(30) Hauer, J.; Buckup, T.; Motzkus, M. *J. Phys. Chem. A* **2007**, *111*, 10517.
(31) Buckup, T.; Hauer, J.; Möhring, J.; Motzkus, M. *Arch. Biochem. Biophys.* **2009**, *483*, 219.
(32) Namboodiri, V.; Namboodiri, M.; Flachenecker, G.; Materny, A. *J. Chem. Phys.* **2010**, *133*, 054503.
(33) Liebers, J.; Scaria, A.; Materny, A.; Kleinekathofer, U. *Phys. Chem. Chem. Phys.* **2010**, *12*, 1351.
(34) Scaria, A.; Liebers, J.; Kleinekathofer, U.; Materny, A. *Chem. Phys. Lett.* **2009**, *470*, 39.
(35) Motzkus, M.; Pedersen, S.; Zewail, A. H. *J. Phys. Chem.* **1996**, *100*, 5620.
(36) Li, C.; Miki, T.; Kakitani, Y.; Koyama, Y.; Nagae, H. *Chem. Phys. Lett.* **2007**, *450*, 112.
(37) Kauppinen, J.; Partanen, J. *Fourier Transforms in Spectroscopy*; Wiley-VCH: Berlin, 2001.
(38) Mukamel, S. *Principles of Nonlinear Optical Spectroscopy*; Oxford University Press: New York, 1995.
(39) Rondonuwu, F. S.; Kakitani, Y.; Tamura, H.; Koyama, Y. *Chem. Phys. Lett.* **2006**, *429*, 234.
(40) McCamant, D. W.; Kukura, P.; Mathies, R. A. *J. Phys. Chem. A* **2003**, *107*, 8208.
(41) Ritz, T.; Damjanovic, A.; Schulten, K.; Zhang, J. P.; Koyama, Y. *Photosynth. Res.* **2000**, *66*, 125.
(42) Papagiannakis, E.; van Stokkum, I. H. M.; Vengris, M.; Cogdell, R. J.; van Grondelle, R.; Larsen, D. S. *J. Phys. Chem. B* **2006**, *110*, 5727.
(43) Vaccaro, P. H. *Advanced series in physical chemistry: Molecular dynamics and spectroscopy by stimulated emission pumping*; World Scientific Publishers: New York, 1994.
(44) Larsen, D. S.; Papagiannakis, E.; van Stokkum, I. H. M.; Vengris, M.; Kennis, J. T. M.; van Grondelle, R. *Chem. Phys. Lett.* **2003**, *381*, 733.
(45) Savolainen, J.; Buckup, T.; Hauer, J.; Jafarpour, A.; Serrat, C.; Motzkus, M.; Herek, J. L. *Chem. Phys.* **2009**, *357*, 181.
(46) Kosumi, D.; Fujiwara, M.; Fujii, R.; Cogdell, R. J.; Hashimoto, H.; Yoshizawa, M. *J. Chem. Phys.* **2009**, *130*, 214506.
(47) Koyama, Y.; Kakitani, Y.; Miki, T.; Christiana, R.; Nagae, H. *Int. J. Mol. Sci.* **2010**, *11*, 1888.